Laser Chem. 1987, Vol. 7, pp. 79–93

Printed in the United Kingdom

A Spectroscopic Study of the $D(0_u^+)$ Ion-pair State of I_2 by Optical–Optical Double Resonance

TAKASHI ISHIWATA and IKUZO TANAKA

Department of Chemistry, Tokyo Institute of Technology, Ohokayama, Meguro, Tokyo 152, Japan

The $D(0_u^+)$ ion-pair state of I_2 has been analyzed by the optical–optical double resonance (OODR) technique. In a stepwise three-photon excitation scheme, $D(0_u^+)$–$B^3\Pi(0_u^+)$–$X^1\Sigma_g^+$, the $D(0_u^+)$ state appeared in the OODR spectrum as the vibrational progressions consisting of O, Q and S branches in accord with the rotational selection rule of $\Delta J = 0$ and ± 2 for the coherent two-photon transition from the $B^3\Pi(0_u^+)$ state. The $D(0_u^+)$–$X^1\Sigma_g^+$ fluorescence was resolved to determine the absolute vibrational numbering of the $D(0_u^+)$ state. We derived Dunham parameters effective for $v = 0$ through $v = 124$ which were used to construct a Rydberg–Klein–Rees (RKR) potential curve.

KEY WORDS: Optical–optical double resonance, I_2; ion-pair state; $D(0_u^+)$ state; two-photon transition.

INTRODUCTION

The study of molecules by multiphoton absorption has recently developed into a significant branch in molecular spectroscopy[1]. One reason is that a spectrum of multiphoton transition often provides the information on electronic states which are normally inaccessible by conventional spectroscopic methods. The technique of choice is optical–optical double resonance (OODR), where the molecular excitation is achieved through a well-defined intermediate state.

In the recent publications of our laboratory[2–4], this new method has been demonstrated to have much advantage for the spectroscopic study of halogen molecules to elucidate their excited states of ion-pair character for several reasons. (1) Since the excitation of molecules proceeds only through appropriate rovibronic levels of the intermediate $B^3\Pi(0_u^+)$ state, the spectra obtained are drastically simplified and easily interpreted. One can easily analyze the rotational energy level of excited states in detail on the basis of the selection rules. (2) The parity selection rule of OODR transitions is different from one-photon process; either the *g* or *u* ion-pair state is detected, depending on whether the total number of photons absorbed are even or odd, respectively. (3) In terms of relative position of the $B^3\Pi(0_u^+)$ intermediate state, the intermediate state can gain its own Franck–Condon region during the excitation. A stepwise process then permits the probing of excited states, direct transitions to which are prohibited by the Franck–Condon principle, as well as by the selection rules in the usual optical transition. This is in sharp contrast with those whose detailed studies of the ion-pair states have been restricted by the spectral congestion and limited resolution available with conventional spectroscopy[5]. In this respect, our studies could solve the problem of multiple excitation of the molecules encountered in the discharge experiments and simple laser excitation studies, clarifying the role of the ion-pair states in the ultraviolet and vacuum ultraviolet emission.

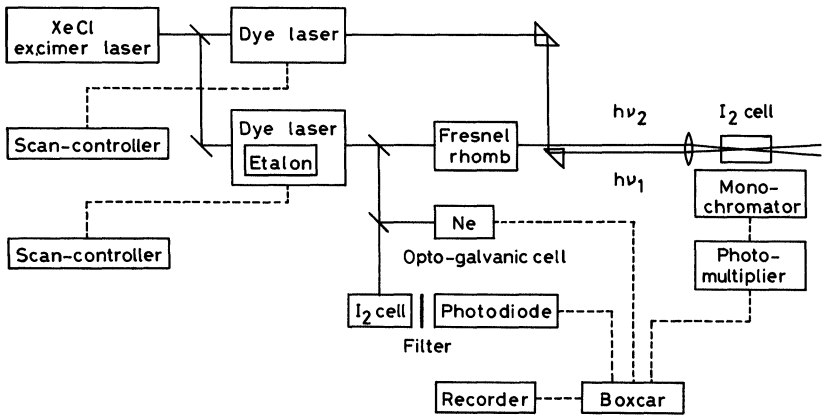

Figure 1 Schematic diagram of the experimental setup for the double resonance spectroscopy.

In this paper we present the results of the OODR analysis on the $D(0_u^+)$ ion-pair state of I_2 which correlates with $I^-(^1S) + I^+(^3P_2)$ at the dissociation limit. The observations were made on the vibrational levels of $v' = 0$ through $v' = 124$ corresponding to about one-third of the dissociation energy of the $D(0_u^+)$ state. A set of molecular constants in a Dunham-type expression is given as well as an RKR potential curve. The assignments of double resonance transitions were performed on the basis of the rotational selection $\Delta J = 0, \pm 2$ for the $D(0_u^+)$–$B^3\Pi(0_u^+)$ two-photon transition, in accord with the excitation scheme; $D(0_u^+)$–$B^3\Pi(0_u^+)$–$X^1\Sigma_g^+$. The absolute vibrational numbering of the $D(0_u^+)$ state was established from a characteristic intensity pattern of the $D(0_u^+)$–$X^1\Sigma_g^+$ emission spectrum on the basis of the Franck–Condon factor calculations.

EXPERIMENTAL DETAILS

Figure 1 shows a schematic diagram of the experimental setup used in this study. An output of pulsed XeCl excimer laser (Lambda Physik EMG 103–MSC) was divided by a beam splitter to pump two tunable dye lasers of the same type simultaneously (Lambda Physik FL 2002E). Both dye lasers produces the pulses with an energy of around 5–10 mJ/pulse with 15 ns duration in the wavelength range of 865–540 nm by using laser dyes commercially available (Lambda Physik Styryl 9, Pyridin 2, DCM, Rhodamin B, Rhodamin 6G, Coumarin 153). The spectral bandwidth was 0.04 cm^{-1} in the case of operating with an intracavity etalon and 0.2–0.5 cm^{-1} without an etalon. The experiments were performed at a repetition rate of 10 Hz.

The laser beams were aligned to propagate in parallel, and cofocused into a sample cell containing I_2 molecules for excitation to the ion-pair states with ungerade symmetry in a total three-photon process. The principle of experiments is shown in Figure 2. The pump laser ($h\nu_1$) operated at the fixed frequency was used to pump the molecules from the ground $X^1\Sigma_g^+$ state to an appropriate rovibronic level of the $B^3\Pi(0_u^+)$ state as an intermediate. The $B^3\Pi(0_u^+)$–$X^1\Sigma_g^+$ transitions were selected by monitoring its near infrared emission and assigned by using their well-known molecular constants. The probe laser ($h\nu_2$) was then scanned to probe the ion-pair states in a coherent two-photon transition. The OODR signals were detected by the use of

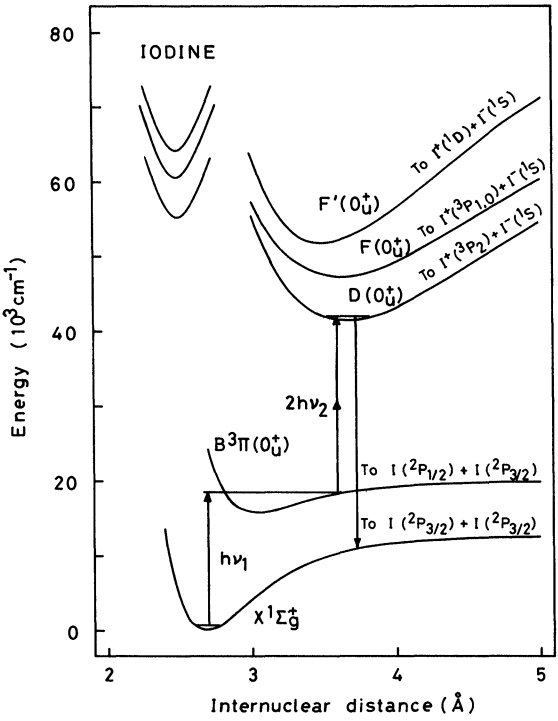

Figure 2 Schematic energy level diagram for the principle of the double resonance experiment on the $D(0_u^+)$ ion-pair state of I^2.

ultraviolet fluorescence terminating in the $X^1\Sigma_g^+$ ground state through a band-pass filter (Corning 7–54) or monochromator. A photomultiplier's (Hamamatsu Photonics R166UH and R106UH) signals were amplified 10 times by a preamplifier (PAR 115) and were integrated by a boxcar (PAR 162/165).

The probe laser frequencies were calibrated by reference to the $B^3\Pi(0_u^+)$–$X^1\Sigma_g^+$ spectrum of I_2[6], when the intracavity etalon was installed in the dye laser. The spectral position could be determined with an estimated accuracy of $0.02\,cm^{-1}$. When dealing with some OODR transitions below 14,800 cm^{-1}, the standard was replaced by the optogalvanic signal of Ne[7] and the accuracy of frequency calibration is around 0.3 cm^{-1} in this case.

The output of dye lasers was vertically polarized in the normal

OODR experiments. In order to examine the anisotropic character of the two-photon transitions originating from the $B^3\Pi(0_u^+)$ state, the polarization angle of the probe laser beam could be changed. The optical components used for this purpose consisted of a polarizer, a double Fresnel rhomb, and a single Fresnel rhomb[8].

In a separate experiment, two laser frequencies were adjusted to excite the desired $D(0_u^+)$–$B^3\Pi(0_u^+)$–$X^1\Sigma_g^+$ transition, and the fluorescence spectrum was recorded by using a 50-cm monochromator (Nikon G–500 with a grating brazed at 300 nm with 1200 grooves/mm).

RESULTS AND DISCUSSION

Optical–optical double resonance transitions

In the present experiments, we have analyzed the energy levels of the $D(0_u^+)$ ion-pair state by the OODR transitions arising from a one-photon resonant three-photon absorption through the $B^3\Pi(0_u^+)$ state as an intermediate.

$$D(0_u^+) \xleftarrow{2h\nu_2} B^3\Pi(0_u^+) \xleftarrow{h\nu_1} X^1\Sigma_g^+ \qquad (1)$$

In general several $B^3\Pi(0_u^+)$–$X^1\Sigma_g^+$ transitions lie near resonance to the pump frequency, while the OODR excitation spectra obtained are quite simple to interpret. The multiple excitation offers no real difficulty in the assignment of spectra, and gives an advantage in the speed of data collection in the analysis of the $D(0_u^+)$ ion-pair state.

Figure 3 shows a part of typical OODR spectrum taken under low resolution. This spectrum was obtained by scanning the probe laser frequency (ν_2) using a sample pressure of around 0.3 Torr without any time delay between pump and probe laser pulses. The pump laser frequency (ν_1) was adjusted to a photon energy of 17 306.3 cm^{-1}, which is in resonance with the three rotational lines of the $B^3\Pi(0_u^+)$–$X^1\Sigma_g^+$ transition within the laser bandwidth: $(14\text{–}0)P_{27}$ and R_{32}, and $(15\text{–}0)R_{102}$. The I_2 emission was then monitored through a monochromator at 320 nm with 10-nm resolution, where the strong $D(0_u^+)$–$X^1\Sigma_g^+$ fluorescence was reported in the discharge experiments[9,10]. The probe laser was operated with (*a*) vertical and (*b*) circular polarization, where the pump laser was vertically polarized. These spectra are drawn on the same scale for comparison.

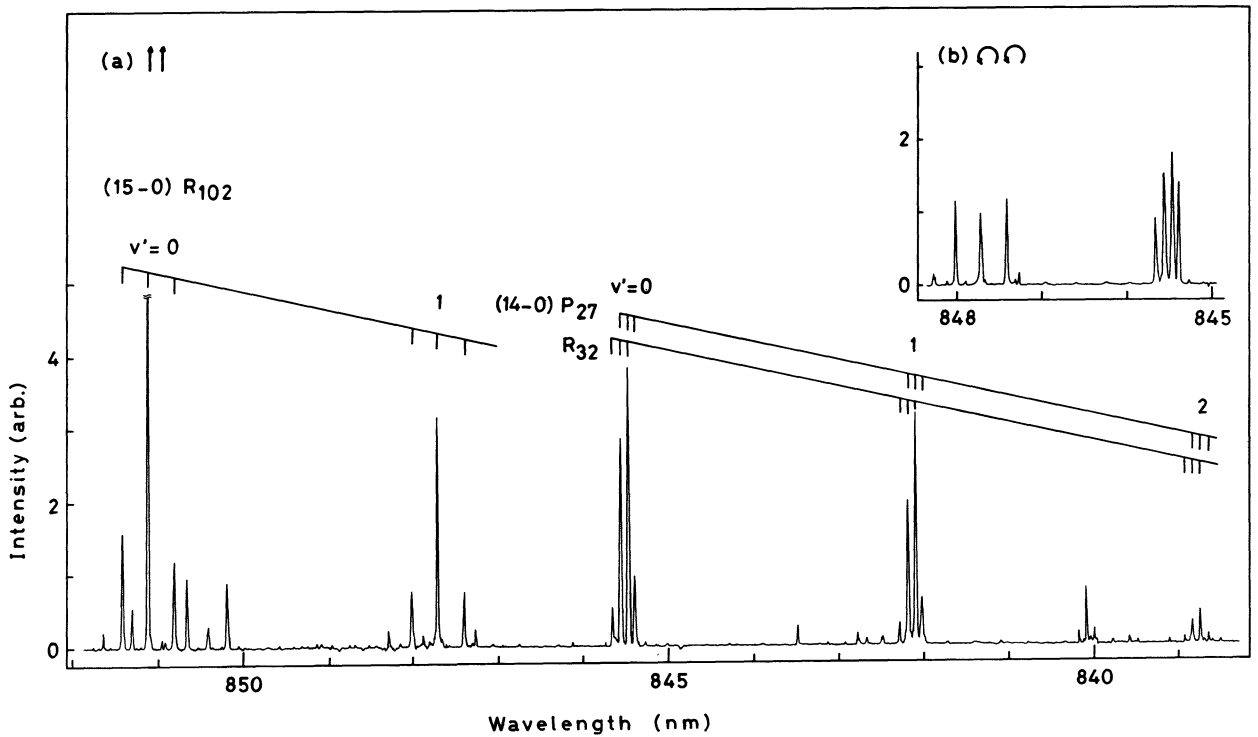

Figure 3 A typical example of the optical–optical double resonance spectra, showing the $D(0_u^+)$ state of I_2. The pump frequency was tuned to the (14–0) P_{27} and R_{32}, and R_{102} transitions of the $B^3\Pi(0_u^+)$–$X\Sigma_g^+$ system. The two-photon transitions originated from the $B^3\Pi(0_u^+)$ state by the probe laser alone and were assigned in accord with the selection rule of the $D(0_u^+)$–$B^3\Pi(0_u^+)$ transition, $\Delta J = 0, \pm 2$. The absolute v' numbering was determined from the emission spectrum on the basis of the Franck–Condon factor calculations. (a) Both the pump and probe lasers were vertically polarized. The same spectrum was obtained, when the probe laser was changed to horizontal polarization. (b) The probe laser was operated with circular polarization, while the pump laser was vertically polarized.

Under our experimental conditions, the rotational relaxation of I_2 in the intermediate $B^3\Pi(0_u^+)$ state does not occur during a stepwise excitation. The OODR transitions reflect the rotational levels of the intermediate $B^3\Pi(0_u^+)$ state, from which a coherent two-photon transition originates. For example, a Fortrat diagram of the (84–15) $D(0_u^+)$–$B^3\Pi(0_u^+)$ transition is shown in Figure 4. Three rotational transitions appeared in any OODR excitation spectra, and their profiles were not affected by a change of the (v, J) levels of the intermediate $B^3\Pi(0_u^+)$ state. However, it should be pointed out here that the individual line intensities of three rotational transitions change with the different mode of polarization. When the polarization of the probe laser was changed from linear to circular, the intensity of the dominant branch in the middle dropped to about one-quarter. It became even smaller than the adjacent two branches which increased in their intensities by about 50%, a typical example of which is shown in Figure 3b. When the probe laser was changed to horizontal polarization, the same spectrum as that shown in Figure 3a was obtained. This is because the randomly oriented molecules cannot distinguish

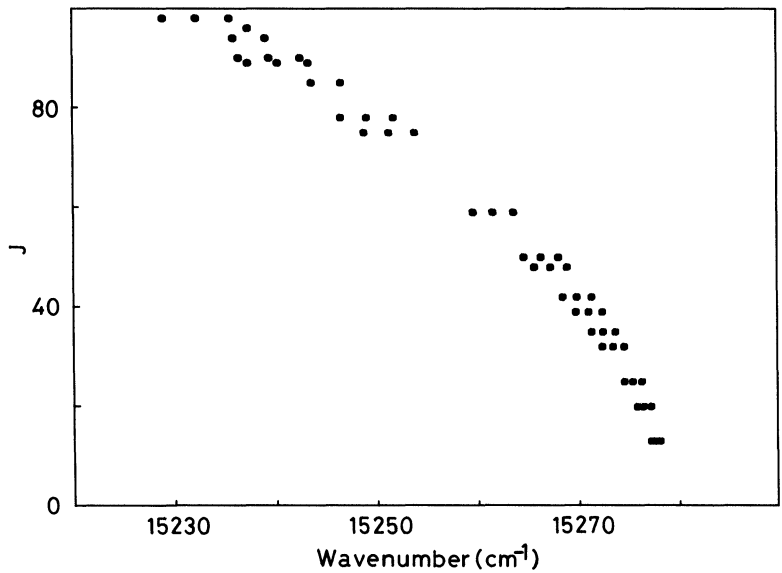

Figure 4 A Fortrat diagram of the (84–15) $D(0_u^+)$–$B^3\Pi(0_u^+)$ two-photon transition.

the horizontal polarized photons from the vertical ones in a coherent two-photon transition induced by the same incident photons of the probe laser.

The pattern of a two-photon absorption is closely related to the rotational selection rule and the anisotropic character of transition strengths is important to establish the transition originating from the intermediate $B^3\Pi(0_u^+)$ state under the study. The possible excited states which can be combined with the $B^3\Pi(0_u^+)$ state by a coherent two-photon transition of identical photons are 0_u^+, 1_u and 2_u in Hund's case *c* notation. According to the discussion of McClain and Harris[11], the rotational selection rules are:

$$\Delta J = 0 \text{ and } \pm 1 \qquad \text{for } 0^+ - 0^+ \text{ transition} \tag{2}$$

$$\Delta J = 0, \pm 1 \text{ and } \pm 2 \qquad \text{for } 1 - 0^+ \text{ and } 2 - 0^+ \text{ transitions,} \tag{3}$$

where the strengths (δ) of coherent two-photon transition depend on (*a*) a factor specified by J'' and J', analogous to the Hönl–London factors of one-photon transition, (*b*) an intrinsic factor characteristic of the particular vibronic transition, and (*c*) a factor dependent on the polarization vector of two photons absorbed simultaneously. In the case of the 0^+–0^+ transition, the transition strength ratio is simply expressed as

$$\delta_{cc}/\delta_{ll} = 3/2 \qquad \text{for } O \text{ and } S \text{ branches,} \tag{4}$$

where subscript l and c designate linearly and circularly polarized photons, respectively. For the *Q* branch, the intensity ratio is known to depend on the type of transition. The ratio of δ_{cc}/δ_{ll} = 1/3 –1/5 are expected from our experience of the study on the ion-pair state of halogen molecules. In the $1 - 0^+$ transitions, the intensities of the *Q* branch rapidly decrease with increasing *J*. The *Q*, *P*, *R* and *S* branches are dominant with almost the same intensities at high *J* levels. The ratio of the transition strength of circular polarized light to that of linearly polarized light (δ_{cc}/δ_{ll}) is 3/2 for all the branches. In the $2 - 0^+$ transitions, the *O*, *P*, *Q*, *R* and *S* branches appear in the ratio of 1 : 4 : 6 : 4 : 1 at high *J* levels and the ratio of δ_{cc}/δ_{ll} is also 3/2 for all of these branches.

The appearance of three rotational lines in the OODR spectrum is consistent with the symmetry of the $D(0_u^+)$ ion-pair state, and they can be attributed to *O*, *Q* and *S* branches in order with an increase of the

probe laser frequency. The prediction for the polarization effects of incident photons on the $D(0_u^+)$–$B^3\Pi(0_u^+)$ transition strengths agrees with our observations, indicating that the coherent two-photon transition is achieved by the probe laser alone.

Analysis

The molecular constants of the $D(0_u^+)$ state were obtained from a term value analysis. For this purpose, the probe laser frequencies (ν_2) measured are converted to energies which all refer to the potential minimum of the $X^1\Sigma_g^+$ ground state ($T_{v',J}^D$) by

$$T_{v',J}^D = h\nu_1 + 2h_{\nu 2} + G''(v) + F'_v(J). \tag{5}$$

The pump frequency (ν_1) and the term value of the ground state ($G''(v) + F'_v(J)$) were calculated from the constants derived by Luc from the $B^3(0_u^+)$–$X^1\Sigma_g^+$ absorption spectrum. At this time, the assignment of the $D(0_u^+)$ state appearing in the OODR spectra was straightforward from the selection rule of $\Delta J = 0$ and ± 2, because the rotational of the pumped $B^3\Pi(0_u^+)$ state was known for each set of experiments†.

On the other hand, the absolute vibrational numbering of the $D(0_u^+)$ state was established from the emission spectrum shown in Figure 5. This spectrum was obtained when the probe laser frequency was tuned to a Q branch which is involved in the first member of the vibrational progression observed through the $(14\text{–}0)R_{32}$ $B^3\Pi(0_u^+)$–$X^1\Sigma_g^+$ pump transition. Even though the expected P and R branches are not resolved in the spectrum, the absolute wavelength position of the $D(0_u^+)$–$X^1\Sigma_g^+$ transition were calculated to assign the spectrum by using the molecular constants of the $^1\Sigma_g^+$ state[13]. The calculations are consistent with the spectral positions of observed vibrational progression and the results are shown in Figure 5. Since the internuclear distance of ion-pair states of I_2 is much longer (typically $r_e = 3.6$ Å) than that of the ground state ($r_e = 2.67$ Å), the transition terminates on the high vibrational levels, as expected. In this case, the Franck–Condon principle indicates that the low-v' levels of the ion-pair states display in

† The pump transitions used in the experiments are as follows: (13–0) P_{48}, R_{53}, P_{60}, R_{65}, (14–0) P_{27}, R_{32}, R_{95}, R_{98}, (15–0) P_{14}, R_{19}, P_{26}, R_{31}, P_{33}, P_{36}, R_{38}, R_{41}, P_{51}, P_{60}, R_{74}, P_{79}, R_{84}, R_{89}, P_{90}, R_{93}, R_{95}, R_{97}, R_{129}, (16–0) P_{19}, P_{91}, (61–1) R_{90}, (17–0) P_{87}, P_{92}, (18–0) P_{124}, (22–0) P_{73}, R_{77}, (26–0) P_{29}, P_{55}, R_{77}, (27–0) P_{79}, (29–1) R_{44}, (31–0) P_{50}, R_{53}, (33–0) P_{49}, (34–0) P_{33}, R_{36}, R_{73}, P_{79}, (35–0) R_{95}, (37–0) P_{127}.

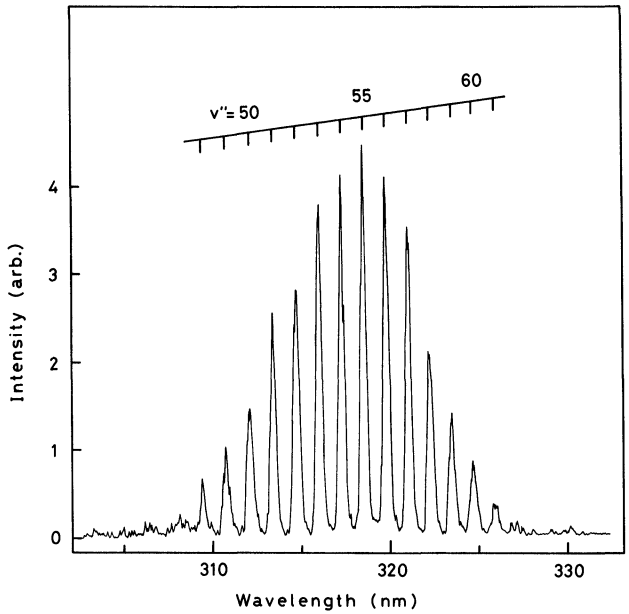

Figure 5 The $D(0_u^+)$–$X^1\Sigma_g^+$ fluorescence spectrum of I_2 (uncorrected for the spectral sensitivity of the detection system. The excitation process is

$$D(0_u^+) \xleftarrow[(0\text{–}14)Q_{33}]{2h\nu_2} B^3\Pi(0_u^+) \xleftarrow[(14\text{–}0)R_{32}]{h\nu_1} X^1\Sigma_g^+$$

The Franck–Condon factors calculated for this transition are as follows:

v	42	43	44	45	46	47	48	49	50	51	52
FCF(10^{-4})	1	3	8	19	41	82	154	271	443	666	919
	53	54	55	56	57	58	59	60	61	62	63
	1157	1319	1351	1229	981	676	395	190	72	20	4

emission a band system whose intensity distribution is modulated according to the probability distribution of the upper vibrational wavefunction. It should be noted that an envelope of emission spectrum in Figure 5 shows a single intensity maximum, indicating that the fluorescence originates from a $v' = 0$ level. This view is also supported by the fact that the double resonance signal suddenly breaks off at the

Table I Dunham parameters of the $D(0_u^+)$ ion-pair state of I_2[a]

Y_{00}	=	41 028.584(47)[b]
Y_{10}	=	94.9928(60)
Y_{20}	=	−0.10919(26)
Y_{30}	=	$-5.805(50) \times 10^{-4}$
Y_{40}	=	$3.686(43) \times 10^{-6}$
Y_{50}	=	$7.61(13) \times 10^{-9}$
Y_{01}	=	0.0207149(64)[c]
Y_{11}	=	$-4.374(38) \times 10^{-5}$
Y_{21}	=	$-8.99(79) \times 10^{-8}$
Y_{31}	=	$6.58(48) \times 10^{-10}$
Y_{02}	=	$-4.93(27) \times 10^{-9}$

[a] Effective for $v = 0$ throught $v = 124$.
[b] Values in parentheses denote one standard deviation and should apply to the last digits of constants.
[c] Equilibrium internuclear distance is calculated as $r_e = 3.583$ Å.

longer wavelength end of the vibrational progression, as shown in Figure 3.

The term values of the $D(0_u^+)$ state were then submitted to a global least-squares fit to the Dunham expansion:

$$T_{v,J}^{D} = \sum_{k,n} Y_{nk}(v + \tfrac{1}{2})^n J^k (J + 1)^k \tag{6}$$

The data include 1593 OODR transitions with $0 \leq v \leq 124$ and $11 \leq J \leq 132$, in which 297 data were measured under high resolution by installing an intracavity etalon in the probe laser. The fitting of level energies required 11 parameters as listed in Table I, and the analysis involving any other parameters of higher-order did not show drastic improvement in the fitting. In the calculations, we weighted the 1296 low-resolution data by a factor of 0.1, since the observed frequency uncertainty is almost an order of magnitude larger than that for high-resolution data. The standard deviation of the global fits is 0.052 cm^{-1} for $76 \leq v \leq 124$ and 0.31 cm^{-1} below this limit. The coefficients in Table I can be used to regenerate all $D(0_u^+)$ term values in the fitted range to 0.9 cm^{-1}†.

† The value of Y_{02} derived from the relation of $Y_{02} = -4Y_{01}^3/Y_{10}^2 (= -3.94 \times 10^{-9}\,cm^{-1})$ is about 20% smaller than that derived by global fitting, since this higher order constant is almost determined from the OODR transitions to the higher v' levels. For example, the OODR transitions shown in Figure 3 was fitted to the customary formula, $T_{v',J}^{D} = T_v + B_v J(J + 1) - D_v J^2(J + 1)^2$, describing the energy levels of the $D(0_u^+)$ $v = 84$ state. We obtained $T_v = 48\,080.702(2)$, $B_v = 0.0167762(15)$, and $D_v = 4.58(15) \times 10^{-9}$ (all in cm^{-1} and one standard deviations in parentheses) with $\delta_{fit} = 0.012\ cm^{-1}$.

The molecular contents in Table I used to construct an RKR potential curve of the $D(0_u^+)$ state[14]. The RKR turning points of the $J = 0$ levels, $U_0(r)$, are summarized for the observed vibrational levels in Table II. On the other hand, the molecular constants of the $X^1\Sigma_g^+$ state have been determined in great detail. We have then calculated the

Table II RKR potential curve of the $D(0_u^+)$ ion-pair state.

v	T_v(cm^{-1})	B_v(cm^{-1})	Turning points (Å) Inner	Outer
-0.5	0.0		3.583	
0	47.47	0.020693	3.508	3.658
1	142.24	649	.458	.717
2	236.79	605	.424	.759
3	331.12	561	.397	.794
4	425.21	516	.374	.825
5	519.07	472	.355	.853
6	612.69	427	.337	.880
7	706.07	382	.320	.904
8	799.22	337	.306	.928
9	892.11	292	.292	.950
10	984.76	246	.279	.972
11	1077.16	201	.266	.992
12	169.31	155	.255	4.013
13	261.20	110	.244	.032
14	352.83	064	.233	.051
15	444.20	018	.223	.070
16	535.31	0.019972	.214	.088
17	626.16	925	.204	.106
18	716.74	879	.196	.124
19	807.05	833	.187	.141
20	897.09	786	.179	.158
21	986.86	739	.171	.175
22	2076.35	693	.163	.192
23	165.57	646	.156	.208
24	254.51	599	.148	.225
25	343.17	552	.141	.241
26	431.55	505	.134	.257
27	519.65	458	.128	.273
28	607.46	410	.121	.288
29	694.99	363	.115	.304
30	782.23	316	.109	.319
31	869.18	268	.103	.334
32	955.85	221	.097	.350
33	3042.22	173	.091	.365
34	128.30	126	.085	.380
35	214.10	078	.080	.395
36	299.59	030	.075	.409
37	384.80	0.018983	.069	.424
38	469.71	935	.064	.439
39	554.32	887	.059	.454
40	638.64	840	.054	.468
41	722.66	792	.049	.483
42	806.38	744	.044	.497
43	889.81	696	.040	.511
44	972.93	648	.035	.526
45	4055.76	600	.030	.540
46	138.29	553	.026	.554
47	220.51	505	.022	.569
48	302.44	457	.017	.583
49	384.07	409	.013	.597
50	465.39	361	.009	.611
51	546.41	314	.005	.625
52	627.14	266	.001	.639
53	707.56	218	2.997	.653
54	787.68	170	.993	.667
55	867.50	123	.989	.681
56	4947.02	0.018075	2.985	4.695
57	5026.23	028	.981	.709
58	105.15	0.017980	.977	.723
59	183.76	932	.974	.737
60	262.07	885	.970	.751
61	340.08	838	.967	.765
62	417.79	790	.963	.779
63	495.20	743	.960	.792
64	572.31	696	.956	.806
65	649.12	649	.953	.820
66	725.63	602	.949	.834
67	801.85	555	.946	.848
68	877.76	508	.943	.862
69	953.37	461	.939	.875
70	6028.69	415	.936	.889
71	103.71	368	.933	.903
72	178.43	322	.930	.917
73	252.86	275	.927	.930
74	326.99	229	.924	.944
75	400.82	183	.921	.958
76	474.36	137	.918	.972
77	547.61	091	.915	.985
78	620.56	045	.912	.999
79	693.22	000	.909	5.013
80	765.58	0.016954	.906	.027
81	837.66	909	.903	.041
82	909.44	864	.900	.054
83	980.94	819	.897	.068
84	7052.14	774	.895	.082
85	123.06	729	.892	.096
86	193.69	684	.889	.109
87	264.03	640	.886	.123
88	334.08	596	.884	.137
89	403.85	551	.881	.151
90	473.34	508	.878	.164
91	542.54	464	.876	.178
92	611.45	420	.873	.192
93	680.09	377	.870	.206
94	748.44	334	.868	.220
95	816.51	291	.865	.233
96	884.30	248	.863	.247
97	951.81	205	.860	.261
98	8019.05	163	.858	.275
100	152.68	079	.853	.303
102	285.21	0.015995	.848	.330
104	416.64	913	.843	.358
106	546.98	831	.838	.386
108	676.23	751	.833	.414
110	804.40	671	.828	.441
112	931.50	593	.824	.469
114	9057.53	515	.819	.497
116	182.49	439	.814	.525
118	306.40	364	.810	.553
120	429.26	290	.805	.581
122	551.06	217	.800	.609
124	671.82	145	.796	.637

Franck–Condon factors of the transition between the $X^1\Sigma_g^+$ and $D(0_u^+)$ states to confirm the intensity distribution of the emission spectrum in Figure 5. The calculation was made on the basis of the effective potential curves for the corresponding J levels, $U_J(r) = U_0(r) + J(J+1)\hbar/2\mu r$, where the emission was observed. It is obvious the observed band shape were fairly consistent with the calculations.

Ion-pair state

The ultraviolet emission of I_2 has recently been analyzed through conventional spectroscopy under high resolution and by optical–optical double resonance method. Of particular interest in these studies is the identification of the ion-pair states correlating with $I^-(^1S) + I^+(^3P, ^1D, ^1S)$. A reliable model regarding their electronic structure is now presented both from experimental[4,15–21] and theoretical sides[22]. Table III summarizes their spectroscopic data available up to date. The six states [$(D'(2_g)$, $\beta(1_g)$, $E(0_g^+)$, $\delta(2_u)$, $\gamma(1_u)$, and $D(0_u^+)$] which belong to the lowest group correlating with ionic states of $I^-(^1S) + I^+(^3P_2)$ lie at around 40 000 cm^{-1} above the $X^1\Sigma_g^+$ ground state. The next highest group also involves the six states [$f(0_g^+)$, $F(0_u^+)$, 1_u, 0_u^-, $G(1_g)$ and $g(0_g^-)$] correlating with $I^-(^1S) + I^+(^3P_1, ^3P_0)$ and has been expected to lie at around 47 000 cm^{-1}. Only the $F'(0_u^+)$ state has been identified at around 51 700 cm^{-1} among the six states (2_u, 1_u, 0_u^+, 2_g, 1_g and 0_g^+) correlating with $I^-(^1S) + I^+(^1D)$.

Table III Molecular constants of ion-pair states of I_2 molecule.

State	$T_e(cm^{-1})$	$\omega_e(cm^{-1})$	$r_e(Å)$	Dissociation limit	Reference
$F'(0_u^+)$	51706.2	131.0	3.48	$I^-(^1S) + I^+(^1D)$	4a
$G(1_g)$	47559.1	106.6	3.53	$I^-(^1S) + I^+(^3P_{1,0})$	23
$F(0_u^+)$	47217.4	96.3	3.60		4b
$g(0_g^-)$	47070	105.7	(3.55)[a]		22
$f(0_g^+)$	47025.9	104.2	3.57		21
$\delta(2_u)$	41789	100.2	(4.0)[a]	$I^-(^1S) + I^+(^3P_2)$	20
$\gamma(1^u)$	41612.3	95.0	3.68		20
$E(0_g^+)$	41411.8	101.4	3.65		19
$D(0_u^+)$	41028.6	95.0	3.58		this work
$\beta(1_g)$	40821.0	105.0	3.61		18
$D'(2_g)$	40388.3	104.0	3.61		17

[a] Theoretical value from Jaffe[22].

The $D(0_u^+)$ ion-pair state is responsible for the absorption spectrum between 175 and 200 nm[23,24]. The spectrum shows some discrete band systems, while their analysis suffers from the overlapping problems of many possible transitions due to the high density of states. Furthermore, the transition terminates on the high v' levels in this energy range, making the absolute v' numbering impractical. The $D(0_u^+)$ state has been also studied by the multiphoton ionization experiment[25] and multiphoton absorption measurement[26], although there were no reliable spectroscopic data available until recently. Three years ago, Tellinghuisen reported the emission spectrum of I_2 using Tesla discharge in the presence of Ar, which contains several vibrational progressions originating from the lower vibrational levels ($v' = 0$–3) of the $D(0_u^+)$ state[9]. More recently, he examined the McLennan bands on the basis of the quantum simulations of the $D(0_u^+)$–$X^1\Sigma_g^+$ emission, giving an improved description of the $D(0_u^+)$ state[10]. His recommended spectroscopic parameters of $T_e = 41\,026.4 \pm 0.4\,cm^{-1}$, $\omega_e = 95.66 \pm 0.22\,cm^{-1}$, and $r_e = 3.576 \pm 0.015$ Å are very close to our results. The synthetic errors for level energies are within $3\,cm^{-1}$ in the range of $v = 0$ through $v = 124$, where our constants are effective.

CONCLUSION

In closing, our recent optical–optical double resonance studies permit a much more complete description of ion-pair states in halogen molecules than that attained up to the present. However, there still remain a number of problems to be solved. For example, we have observed some effects of interaction between ion-pair states, although the source of perturbation was not always clear due to the lack of sufficient data. Some ion-pair states only appear in the spectrum by the mixing of the wavefunction with the ion-pair state optically allowed from the $B^3\Pi(0_u^+)$ state. As one possible solution, we can use other lower-lying valence states as an intermediate before the $B^3\Pi(0_u^+)$ state to elucidate unknown ion-pair states. These types of experiment are now in progress.

References

1. S. H. Lin, Y. Fujimura, H. J. Neusser, and E. W. Schlag, Multiphoton spectroscopy of molecules. In *Quantum Electronics—Principles and Applications,* Eds P. F. Liao and P. Kelley. (Academic Press, Oriando, Florida: 1984.)

2. (a) T. Ishiwata, I. Fujiwara, T. Shinzawa, and I. Tanaka, *J. Chem. Phys.* **79**, 4779 (1983). (b) T. Ishiwata, T. Shinzawa, T. Kusayanagi, and I. Tanaka, *J. Chem. Phys.* **82**, 1788 (1985). (c) T. Shinzawa, A. Tokunaga, T. Ishiwata, and I. Tanaka, *J. Chem. Phys* **83**, 5407 (1985).
3. (a) T. Ishiwata, A. Tokunaga, T. Shinzawa, and I. Tanaka, *Bull Chem. Soc. Jpn.* **57**, 1317 (1984). (b) T. Shinzawa, A. Tokunaga, T. Ishiwata, I. Tanaka, K. Kasatani, M. Kawasaki, and H. Sato, *J. Chem. Phys.* **80**, 5909 (1984). (c) T. Ishiwata, H. Ohtoshi, and I. Tanaka, *J. Chem. Phys.* **81**, 2300 (1984). (d) T. Ishiwata, A. Tokunaga, T. Shinzawa, and I. Tanaka, *J. Mol. Spectrosc.* **108**, 314 (1984).
4. (a) T. Ishiwata, A. Tokunaga, T. Shinzawa, and I. Tanaka, *J. Mol. Spectrosc.* **117**, 89 (1986). (b) T. Ishiwata, T. Kusayanagi, T. Hara, and I. Tanaka, *J. Mol. Spectrosc.*, in press.
5. K. P. Huber and G. Herzberg *Molecular Spectra and Molecular Structure IV. Constants of Diatomic Molecules*. (Van Nostrand Reinhold Company, New York: 1979.)
6. S. Gerstenkorn and P. Luc, *Atlas du Spectre d'Absorption de la Molécule l'Iode.* Paris, CNRS: (1978).
7. G. R. Harrison, *M.I.T. Wavelength Table.* the M.I.T. Press (1969).
8. B. Rossi, *Optics.* (Addison-Wesley, Reading Mass: 1965).
9. J. Tellinghuisen, *Chem. Phys. Lett.* **99**, 373 (1983).
10. J. Tellinghuisen, *Can. J. Phys.* **62**, 1933 (1984).
11. W. M. McClain and R. A. Harris, *Excited States,* Vol. 1, pp. 1. Ed. E. C. Lim, Academic Press, New York. (1978).
12. P. Luc, *J. Mol. Spectrosc.* **80**, 41 (1980).
13. J. Tellinghuisen, M. R. KcKeever, and A. Sur, *J. Mol. Spectrosc.* **82**, 225 (1980).
14. We have used the version from Hougen of the RKR and FCF program originally written by Zare, Schmeltekopf, Harrop, and Albritton for use in their article in *J. Mol. Spectrosc.* **46**, 37 (1973).
15. J. Tellinghuisen, *J. Mol. Spectrosc.* **94**, 231–252 (1982); *J. Chem. Phys.* **78**, 2374–2380 (1984).
16. J. P. Perrot, M. Broyer, J. Chevaleyre, and B. Femelat, *J. Mol. Spectrosc.* **98**, 161–167 (1983).
17. J. C. D. Brand, A. R. Hoy, A. K. Kalkar, and A. B. Yamashita, *J. Mol. Spectrosc.* **95**, 350 (1983).
18. G. W. King, I. M. Littlewood, and J. R. Robins, *Chem. Phys.* **56**, 145 (1981).
19. J. C. D. Brand and A. R. Hoy, *J. Mol. Spectrosc.* **97**, 379 (1983).
20. K. S. Viswanathan and J. Tellinghuisen, *J. Mol. Spectrosc.* **101**, 285 (1983).
21. K. Wieland, J. Tellinghuisen and A. Nobs, *J. Mol. Spectrosc.* **41**, 69 (1972).
22. R. L. Jaffe, private communication cited in ref. 22.
23. P. Venkateswarlu, *Can. J. Phys.* **48**, 1055 (1970).
24. R. J. Donovan, B. V. O'Grady, K. Shobatake, and A. Hiraya, *Chem. Phys. Lett.* **122**, 612 (1985).
25. K.-M. Chen, L. E. Steenhoek, and E. S. Yeung, *Chem. Phys. Lett.* **59**, 222 (1978).
26. A. D. Williamson and R. N. Compton, *Chem. Phys. Lett.* **62**, 295 (1979).